PIPE BRIDGES SUSPENDED ON CABLES IN ARBITRARY PLANES

By

Zs. GÁSPÁR

Department of Civil Engineering Mechanics, Technical University, Budapest

(Received July 15, 1976)

Presented by Prof. Dr. S. KALISZKY

1. Introduction

Pipe bridges contain small-size beams beside pipes, therefore vertical and horizontal stiffness is normally increased by stiffening cables, arranged in inclined planes as a rule.

The linear theory being uneconomical for suspended beams, utilization of at least second-order theory is advisable. Among others, VISONTAI [1, 2] reported on the approximate analyses of suspended beams with inclined cable plane and rigidity beam, making the following assumptions for suspended beams stiffened by simple beams of uniform load, and braced with two cables of identical geometry:

- only cables are exposed to constant load, the secondary effect of these cable forces is negligible in occurrence of a horizontal load;
- tie rods may be considered as forming an inextensible suspension sheet;
- horizontal and vertical casual loads are independent to calculate;
- suspension sheet keeps plane after deformation;
- suspension points of the beam are level with the gravity centre.

Here an algorithm based on [3] will be presented, making use of the third-order theory for the cable structures (stiffening cables and pertaining tie rods), and of the second-order theory for the bar system. In this latter, gravity centre and shear centre of bar cross sections are assumed to coincide, but no stipulations are made for the beam section and the load type.

This algorithm has been applied to develop a program in ALGOL language. The processed examples were intended to yield a better picture of the forces and reactions in suspension beams of this kind.

2. Computation procedure

The rigidity beam is simulated as a simple beam of constant cross section made of an ideal elastic material, with ends supported fork-like. The beam section is assumed to have at least two axes of symmetry. This beam is connected by tie rods to an arbitrary number of stiffening cables with both ends fixed. Also cables and tie rods are assumed to be ideal elastic.

To simplify starting data, axis of the rigidity beam exposed to stress and dead load is considered to be straight and parallel to the planes of individual cables and tie rods. The assumptions do not reduce this computation to approximative, since these will be involved in the design of the beam shape during construction, and the cable cut lengths.

For equidistant tie rods exposed to equal tensions, the cable will follow a second-order parabola. Indicating the cable suspension points, the parabola rise and the tension in a single cable length for each cable, node positions, stress-free cable length and cable forces are unambiguously determined.

Rigidity beam is considered as a bar system determined by nodes assumed at tie rod joints, also permanent and casual loads are reduced to these nodes, permitting computation according to [4].

Effect of permanent loads and of forces transmitted from tie rods will be computed first. For these latter, the influence line of forces does not absolutely cross the beam gravity line, hence they have to be reduced to the nodes.

Displacement characteristics of, and stresses in the beam are determined by the displacement method according to the first-order theory. Deducing the corresponding displacements from the nodal co-ordinates determines the shape of the beam to be constructed so as to straighten upon combined effect of permanent load and stress.

Deformation and stresses upon casual load are determined by iteration. Once in each step, state change of the rigidity beam considered as independent of the cables is determined by the second-order theory, and the state change due to joint displacement of cable structures (cable + pertaining tie rods) considered as rigidly supported, by the third-order theory.

Rather than to consider all unbalanced loads in computing the beam state change, iteration convergency is provided by reducing some load components (e.g. forces in direction y or torque moments about the z axis) in proportion to the resistance of the rigidity beam and the whole structure to the corresponding displacement. Thereby the reduced load is transmitted to the beam, and cable force changes due to joint displacements about balance the other loads. (Taking these six ratios as unit and applying a casual load of purely unit components, the rigidity ratio is approximated by the formula $\dfrac{1}{h+1}$ where h is the error of the corresponding load component after the first iterative step.)

Thereafter rigidity beam displacements due to the reduced load are determined according to the second-order theory. First-order rigidity matrix of the bar system is computed according to [4], and the complementary rigidity matrix according to item **3**.

In knowledge of the rigidity beam gravity centre displacement, new co-ordinates of the joints between rigidity beam and tie rods can be determined as described in item **4**. The next step is to compute the joint displacement-induced state change of cable structures independent of the rigidity beam and of each other, according to the third-order theory.

Finally, difference between design load and the load balancing internal beam forces and forces transmitted by tie rods is computed. For a slight deviation from the design load, the procedure is considered as accomplished, else the load difference is considered as a further casual load and the procedure is repeated by reducing the load components in proper proportions.

The scheme of the algorithm is seen in the flow chart.
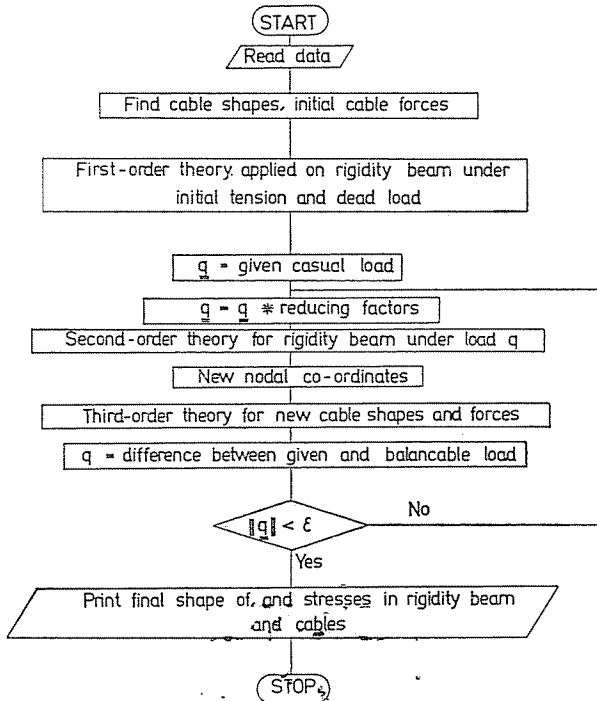
3. Determination of the complementary rigidity matrix

Complementary rigidity matrix of a flexural plane bar is presented in [5]. The relevant procedure will be generalized for spatial bars.

The complementary rigidity matrix $\mathbf{D}$ will be determined from

$$\mathbf{D}\mathbf{u} = -\frac{d}{d\mathbf{u}}\,\Delta\mathbf{u}_2^*\mathbf{r} \tag{1}$$

deduced according to the thesis of potential energy extremum, where $\Delta\mathbf{u}_2$ is a vector containing quadratic terms of displacement $\Delta\mathbf{u}$ due to load variation, and $\mathbf{r}$ is the vector of already developed stresses.
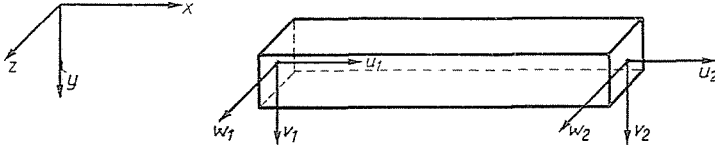

Fig. 1

Secondary energy $\mathcal{L}_r$ can be written as the volume integral of the product of quadratic terms of normal and shear stresses by strain and angular distorsions, respectively. Effect of shear stresses being negligible, and normal stresses arising only in direction x, it can be written:

$$\mathcal{L}_r = -\int_V \sigma_x \varepsilon_{x2}\,dV \tag{2}$$

(with reference systems according to Fig. 1).

Quadratic terms in strain ε_x are given by:

$$\varepsilon_{x2} = \frac{1}{2}\left\{\left(\frac{\partial u}{\partial x}\right)^2 + \left(\frac{\partial v}{\partial x}\right)^2 + \left(\frac{\partial w}{\partial x}\right)^2\right\}. \tag{3}$$

Assuming cross sections normal to the bar axis to be inaffected by deformation, displacements of a cross-section point with co-ordinates (y, z) are:

$$u(x, y, z) = u_0(x) - y\,\frac{\partial v_0(x)}{\partial x} - z\,\frac{\partial w_0(x)}{\partial x}$$

$$v(x, y, z) = v_0(x) \tag{4}$$

$$w(x, y, z) = w_0(x)$$

u_0, v_0, w_0 being displacement functions of bar axis points. From (4a):

$$\left(\frac{\partial u}{\partial x}\right)^2 = \left(\frac{\partial u_0}{\partial x}\right)^2 - 2y\,\frac{\partial u_0}{\partial x}\frac{\partial^2 v_0}{\partial x^2} + y^2\left(\frac{\partial^2 v_0}{\partial x^2}\right)^2 -$$

$$- 2z\,\frac{\partial u_0}{\partial x}\frac{\partial^2 w_0}{\partial x^2} + 2yz\,\frac{\partial^2 v_0}{\partial x^2}\frac{\partial^2 w_0}{\partial x^2} + z^2\left(\frac{\partial^2 w_0}{\partial x^2}\right)^2 \tag{5}$$

(5) substituted into (3):

$$\varepsilon_{x2} = \frac{1}{2}\left\{\left(\frac{\partial u_0}{\partial x}\right)^2 + \left(\frac{\partial v_0}{\partial x}\right)^2 + \left(\frac{\partial w_0}{\partial x}\right)^2\right\} - y\,\frac{\partial u_0}{\partial x}\,\frac{\partial^2 v_0}{\partial x^2} +$$

$$+ \frac{1}{2}\,y^2\left(\frac{\partial^2 v_0}{\partial x^2}\right)^2 - z\,\frac{\partial u_0}{\partial x}\,\frac{\partial^2 w_0}{\partial x^2} + yz\,\frac{\partial^2 v_0}{\partial x^2}\,\frac{\partial^2 w_0}{\partial x^2} + \frac{z^2}{2}\left(\frac{\partial^2 w_0}{\partial x^2}\right)^2.$$

This substituted into (2) and arranged (omitting subscripts 0 of u_0, v_0, w_0):

$$\mathfrak{L}_r = -\int\limits_V \sigma_x \frac{1}{2}\left\{\left(\frac{\partial u}{\partial x}\right)^2 + \left(\frac{\partial v}{\partial x}\right)^2 + \left(\frac{\partial w}{\partial x}\right)^2 +\right.$$

$$\left. + y^2\left(\frac{\partial^2 v}{\partial x^2}\right)^2 + 2xy\,\frac{\partial^2 v}{\partial x^2}\,\frac{\partial^2 w}{\partial x^2} + z^2\left(\frac{\partial^2 w}{\partial x^2}\right)^2\right\}dV + \tag{6}$$

$$+ \int\limits_V z\sigma_x\,\frac{\partial u}{\partial x}\,\frac{\partial^2 w}{\partial x^2}\,dV + \int\limits_V y\sigma_x\,\frac{\partial u}{\partial x}\,\frac{\partial^2 v}{\partial x^2}\,dV.$$

Eq. (6) takes into consideration that:

a) gravity centre displacements are independent of co-ordinates y and z, permitting integration with respect to them;

b) stresses in cross section are given by:

$$N = \int\limits_F \sigma_x dF$$

$$M_v = \int\limits_F z\sigma_x dF \tag{7}$$

$$M_w = \int\limits_F y\sigma_x dF$$

c) $\qquad\qquad \int\limits_F y^2 dF = J_z\,; \qquad\qquad i_z = \sqrt{\dfrac{J_z}{F}}$

$$\int\limits_F z^2 dF = J_y\,; \qquad\qquad i_y = \sqrt{\frac{J_y}{F}}$$

$$\int\limits_F xy\,dF = C_{zy} = 0\,,$$

hence:

$$\mathfrak{L}_r = -\int\limits_l N(x)\frac{1}{2}\left\{\left(\frac{\partial u}{\partial x}\right)^2 + \left(\frac{\partial v}{\partial x}\right)^2 + \left(\frac{\partial w}{\partial x}\right)^2 + i_z^2\left(\frac{\partial^2 v}{\partial x^2}\right)^2 +\right.$$

$$\left. + i_y^2\left(\frac{\partial w}{\partial x^2}\right)^2\right\}dx + \int\limits_l M_v(x)\,\frac{\partial u}{\partial x}\,\frac{\partial^2 w}{\partial x^2}\,dx + \int\limits_l M_w(x)\,\frac{\partial u}{\partial x}\,\frac{\partial^2 v}{\partial x^2}\,dx \tag{8}$$

(8) can be written also as integral of a scalar product:

$$\mathcal{L}_r = - \int_l \Delta \mathbf{v}_2^* \tilde{\mathbf{r}} \, dx \tag{9}$$

where:

$$\tilde{\mathbf{r}}^* = [N(x) \quad M_v(x) \quad M_w(x)] \tag{10}$$

$$\Delta v_2 = \frac{1}{2} \left[\left(\frac{\partial u}{\partial x}\right)^2 + \left(\frac{\partial v}{\partial x}\right)^2 + \left(\frac{\partial w}{\partial x}\right)^2 + i_z^2 \left(\frac{\partial^2 v}{\partial x^2}\right)^2 + i_y^2 \left(\frac{\partial w}{\partial x}\right)^2 \right. \\ \left. - 2 \frac{\partial u}{\partial x} \frac{\partial^2 w}{\partial x^2} \right. \\ \left. - 2 \frac{\partial u}{\partial x} \frac{\partial^2 v}{\partial x^2} \right] \tag{11}$$

Integration in (9) requires assumptions to be made for stress and displacement functions.

For a bar submitted to loads at end points alone and including end-point loads into vector

$$\mathbf{r}^* = [N_0 \quad T_{v0} \quad T_{w0} \quad M_{t0} \quad M_{v0} \quad M_{w0}] \tag{12}$$

functions for stresses in (10) are

$$N(x) = N_0$$
$$M_v(x) = M_{v0} - (l - x)T_{w0} \tag{13}$$
$$M_w(x) = M_{w0} + (l - x)T_{v0} \,.$$

Approximating bar axis displacement functions by functions interpolated between bar end point displacement:

$$u(x) = \mathbf{a}_u^*(x)\mathbf{u}_k$$
$$v(x) = \mathbf{a}_v^*(x)\mathbf{u}_k \tag{14}$$
$$w(x) = \mathbf{a}_w^*(x)\mathbf{u}_k$$

where, denoting $\xi = x/l$

$$\mathbf{u}_k^* = [u_1 \quad v_1 \quad w_1 \quad \varphi_{u1} \quad \varphi_{v1} \quad \varphi_{w1}$$
$$\quad u_2 \quad v_2 \quad w_2 \quad \varphi_{u2} \quad \varphi_{v2} \quad \varphi_{w2}] \tag{15}$$

$$\mathbf{a}_u^* = [1 - \xi \quad 0 \quad 0 \quad 0 \quad 0 \quad 0$$
$$\xi \quad 0 \quad 0 \quad 0 \quad 0 \quad 0]$$

$$\mathbf{a}_v^* = [0 \quad 1 - 3\xi^2 - 2\xi^3 \quad 0 \quad 0 \quad 0 \quad l(\xi - 2\xi^2 + \xi^3)$$
$$0 \quad 3\xi^2 - 2\xi^3 \quad 0 \quad 0 \quad 0 \quad l(-\xi^2 + \xi^3)] \tag{16}$$

$$\mathbf{a}_w^* = [0 \quad 0 \quad 1 - 3\xi^2 - 2\xi^3 \quad 0 \quad l(\xi - 2\xi^2 + \xi^3) \quad 0$$
$$0 \quad 0 \quad 3\xi^2 - 2\xi^3 \quad 0 \quad l(-\xi^2 + \xi^3) \quad 0].$$

Thereby (9) becomes

$$\mathfrak{L}_r = - \int_l \Delta \mathbf{u}_2^* \mathbf{r} \, dx \tag{17}$$

with notations

$$\mathbf{A} = \left\{ \frac{\partial \mathbf{a}_u}{\partial x} \frac{\partial \mathbf{a}_u^*}{\partial x} + \frac{\partial \mathbf{a}_v}{\partial x} \frac{\partial \mathbf{a}_v^*}{\partial x} + \frac{\partial \mathbf{a}_w}{\partial x} \frac{\partial \mathbf{a}_w^*}{\partial x} + \right.$$

$$\left. + i_z^2 \frac{\partial^2 \mathbf{a}_v}{\partial x^2} \frac{\partial^2 \mathbf{a}_v^*}{\partial x^2} + i_y^2 \frac{\partial^2 \mathbf{a}_w}{\partial x^2} \frac{\partial^2 \mathbf{a}_w^*}{\partial x^2} \right\}$$

$$\mathbf{B} = - \left\{ \frac{\partial \mathbf{a}_u}{\partial x} \frac{\partial^2 \mathbf{a}_w^*}{\partial x^2} + \frac{\partial^2 \mathbf{a}_w}{\partial x^2} \frac{\partial \mathbf{a}_u^*}{\partial x} \right\} \tag{18}$$

$$\mathbf{C} = - \left\{ \frac{\partial \mathbf{a}_u}{\partial x} \frac{\partial^2 \mathbf{a}_v^*}{\partial x^2} + \frac{\partial^2 \mathbf{a}_v}{\partial x^2} \frac{\partial \mathbf{a}_u^*}{\partial x} \right\}$$

we obtain:

$$\mathbf{u}_2 = \frac{1}{2} \begin{bmatrix} \mathbf{u}_k^* & \mathbf{A} & \mathbf{u}_k \\ -\mathbf{u}_k^* & (l-x)\,\mathbf{C} & \mathbf{u}_k \\ \mathbf{u}_k^* & (l-x)\,\mathbf{B} & \mathbf{u}_k \\ & \mathbf{0} & \\ \mathbf{u}_k^* & \mathbf{B} & \mathbf{u}_k \\ \mathbf{u}_k^* & \mathbf{C} & \mathbf{u}_k \end{bmatrix}. \tag{19}$$

Comparing (1) and (17) shows feasibility of integrations

$$\mathbf{D} = N_0 \int_0^l \mathbf{A} \, dx + T_{v0} \int_0^l (l-x)\mathbf{C} \, dx - T_{w0} \int_0^l (l-x)\mathbf{B} \, dx + M_{v0} \int_0^l \mathbf{B} \, dx + M_{w0} \int_0^l \mathbf{C} \, dx.$$

Neglecting terms containing inertia radii because of i_y, $i_z \ll l$, $\mathbf{D}$ obtains the form in Table 1. (For simplicity, stress subscripts 0 have been omitted.)

4. Computation of joint co-ordinates

In the initial state, rigidity beam to tie rod joint co-ordinates are known. The presented procedure will be applied to determine rigidity beam nodal displacement components, to yield, in turn, the new joint co-ordinates.

Be $\mathbf{x}_j$ the co-ordinates of the j-th node of the rigidity beam in a known state (maybe the initial one), joined by a tie rod of the k-th cable structure. Co-ordinates of this joint will be included in vector $\mathbf{x}_{jk}$. Relative co-ordinates will be given by:

$$\mathbf{r}_{jk} = \mathbf{x}_{jk} - \mathbf{x}_j.$$

$$
\mathbf{D} = \begin{bmatrix}
\dfrac{N}{l} & -\dfrac{T_v}{l} & +\dfrac{T_w}{l} & T_w-\dfrac{M_v}{l} & -T_v-\dfrac{M_w}{l} & -\dfrac{N}{l} & \dfrac{T_v}{l} & -\dfrac{T_w}{l} & \dfrac{M_v}{l} & \dfrac{M_w}{l} \\[2ex]
 & \dfrac{6N}{5l} & & & \dfrac{N}{10} & \dfrac{T_v}{l} & -\dfrac{6N}{5l} & & & \dfrac{N}{10} \\[2ex]
 & & \dfrac{6N}{5l} & \dfrac{N}{10} & & -\dfrac{T_w}{l} & -\dfrac{6N}{5l} & & \dfrac{N}{10} & \\[2ex]
 & & & \dfrac{2Nl}{15} & & -T_w+\dfrac{M_v}{l} & & -\dfrac{N}{10} & -\dfrac{Nl}{30} & \\[2ex]
 & & & & \dfrac{2Nl}{15} & T_v+\dfrac{M_w}{l} & -\dfrac{N}{10} & & & -\dfrac{Nl}{30} \\[2ex]
 & & & & & \dfrac{N}{l} & -\dfrac{T_v}{l} & +\dfrac{T_w}{l} & -\dfrac{M_v}{l} & \dfrac{M_w}{l} \\[2ex]
\text{Symmetry} & & & & & & \dfrac{6N}{5l} & & & -\dfrac{N}{10} \\[2ex]
 & & & & & & & \dfrac{6N}{5l} & -\dfrac{N}{10} & \\[2ex]
 & & & & & & & & \dfrac{2Nl}{15} & \\[2ex]
 & & & & & & & & & \dfrac{2Nl}{15}
\end{bmatrix}
$$

Table 1.

Including displacement and rotation components of the j-th node of the rigidity beam into vectors $\mathbf{d}$ and $\mathbf{f}$, respectively:

$$\mathbf{d}^* = [u_{jx}u_{jy}u_{jz}], \qquad \mathbf{f}^* = [\varphi_{jx}\varphi_{jy}\varphi_{jz}].$$

Vectors for the new state will be indicated by upper sign $\sim$. $\tilde{\mathbf{x}}_j$ and $\tilde{\mathbf{r}}_{jk}$ will be respective functions of $\mathbf{d}$ and $\mathbf{f}$ alone. The former is easy to obtain from

$$\tilde{\mathbf{x}}_j = \mathbf{x}_j + \mathbf{d}$$

but $\tilde{\mathbf{r}}_{jk}$ is far from being simple to calculate, since the effect of rotations depends on their order, too.

Independent rotations $(\varphi_x, \varphi_y, \varphi_z)$ can be taken into consideration by multiplying vector $\mathbf{r}_{jk}$ by matrices

$$\mathbf{T}_x = \begin{bmatrix} 1 & 0 & 0 \\ 0 & \cos\varphi_x & -\sin\varphi_x \\ 0 & \sin\varphi_x & \cos\varphi_x \end{bmatrix} \qquad \mathbf{T}_z = \begin{bmatrix} \cos\varphi_y & 0 & \sin\varphi_y \\ 0 & 1 & 0 \\ -\sin\varphi_y & 0 & \cos\varphi_y \end{bmatrix}$$

$$\mathbf{T}_z = \begin{bmatrix} \cos\varphi_z & -\sin\varphi_z & 0 \\ \sin\varphi_z & \cos\varphi_z & 0 \\ 0 & 0 & 1 \end{bmatrix} \tag{20}$$

in this order. Multiplying rotations by a scalar parameter $(0 \leq t \leq 1)$ their combined effect can be accounted for by continuously varying the parameter t. Now, $\tilde{\mathbf{r}}_{jk}$ is obtained by numerically integrating an equation of the form:

$$\tilde{\mathbf{r}}_{jk} = \mathbf{r}_{jk} + \int_0^l \mathbf{f}(\mathbf{r}_{jk}(t))dt. \tag{21}$$

Rotation relationships being themselves not perfectly exact (the superposition principle being valid), and the rotations being little, instead of Eq. (21), the effect of rotations will be accounted for in a predetermined order.

$$\tilde{\mathbf{r}}_{jk} = \mathbf{T}_z\mathbf{T}_y\mathbf{T}_z\mathbf{r}_{jk}.$$

Thus, the new co-ordinates of joints will be given by:

$$\tilde{\mathbf{x}}_{jk} = \mathbf{x}_j + \mathbf{d} + \mathbf{T}_z\mathbf{T}_y\mathbf{T}_x\mathbf{r}_{jk}.$$

A third possibility to account for the rotations is to determine the influence line of vector $\mathbf{f}$, and to rotate vector $\mathbf{r}_{jk}$ by a value $|\mathbf{f}|$ around it as an axis. This method is advantageous by being independent of the chosen reference system but the final result cannot be considered as exact either, components of $\mathbf{f}$ having been considered as independent, at the same time it is more labour-consuming than the former method.

5. Numerical results

The presented algorithm has been applied to make a program for the computer ODRA-1204 of the Faculty of Civil Engineering of this University, for processing one of the examples in [1].

Starting data were (according to notations in Fig. 2):

$l = 90.00$ m

$f = 13.50$ m
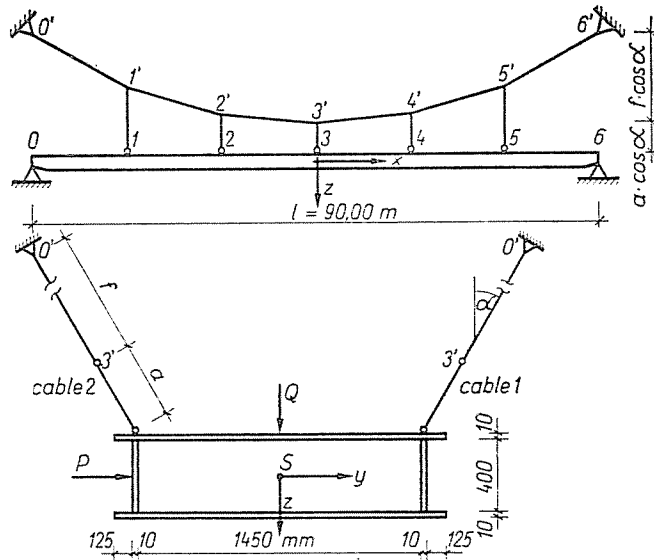
Fig. 2

$\alpha = 30°$

$p = 0.15$ Mp/m

$EA_{\text{cable}} = 13\ 750$ Mp

$EA_{\text{beam}} = 890\ 400$ Mp

$GJ_x = 30\ 600$ m²Mp

$EJ_y = 32\ 500$ m²Mp

$EJ_z = 268\ 000$ m²Mp.

In addition, some data lacking from the approximation [1] had to be assumed:

— number of tie rods for each cable ($n = 5$)

— tie rod stiffness ($EA_f = EA_{\text{cable}}$)

— length of the shortest tie rod ($a = 2$ m)

— initial cable forces (10 Mp in the tie rods)

— vertical projection of the distance between tie rod joints and rigidity beam gravity centres (0.21 m).

The obtained nodal co-ordinates of cable 1 under dead load (those for cable 2 changing only by the sign of y) are shown in Table 2, and cable forces equal in both cables, as well as stress-free lengths have been compiled in Table 3.

Distributed beam load p is reduced to nodes, hence forces $P_y = 2.25$ Mp act at nodes 1 to 5. Nodal co-ordinates and stresses under this load are computed.

New nodal co-ordinates of the cable structure, rope forces, rigidity beam node co-ordinates, axis rotations and individual rod stresses have been compiled in Tables 4, 5, 6 and 7, respectively (symmetric parts being indicated but once).

Table 2

i	$x_i[m]$	$y_i[m]$	$z_i[m]$
0'	-45	8.5101	-13.6333
1'	-30	4.7601	$-\ 7.1381$
2'	-15	2.5100	$-\ 3.2410$
3'	0	1.7600	$-\ 1.9420$
4'	15	2.5100	$-\ 3.2410$
5'	30	4.7601	$-\ 7.1381$
6'	45	8.5101	-13.6333
1	-30	0.7600	$-\ 0.2100$
2	-15	0.7600	$-\ 0.2100$
3	0	0.7600	$-\ 0.2100$
4	15	0.7600	$-\ 0.2100$
5	30	0.7600	$-\ 0.2100$

Table 3

i	j	$s_{ij}[\mathrm{Mp}]$	$l_{ij}[m]$
0'	1'	55.9017	16.7026
1'	2'	52.2015	15.6012
2'	3'	50.2494	15.0199
3'	4'	50.2494	15.0199
4'	5'	52.2015	15.6012
5'	6'	55.9017	16.7026
1	1'	10.0000	7.9941
2	2'	10.0000	3.4974
3	3'	10.0000	1.9985
4	4'	10.0000	3.4974
5	5'	10.0000	7.9941

3

Table 4

i	Cable 1			Cable 2		
	x_i	y_i	z_i	x_i	y_i	z_i
$0'$	-45.0000	8.5101	-13.6333	-45.0000	-8.5101	-13.6333
$1'$	-29.9928	4.8180	-7.1456	-30.0071	-4.7021	-7.1313
$2'$	-14.9934	2.6154	-3.2518	-15.0065	-2.4045	-3.2315
$3'$	0.0000	1.8857	-1.9520	0.0000	-1.6341	-1.9333
1	-30.0034	0.8344	-0.2090	-29.9966	-0.6856	-0.2118
2	-15.0019	0.8876	-0.2085	-14.9981	-0.6324	-0.2129
3	0.0000	0.9066	-0.2083	0.0000	-0.6134	-0.2132

Table 5

i	j	Cable 1	Cable 2
$0'$	$1'$	48.1989	63.6084
$1'$	$2'$	45.0455	59.3500
$2'$	$3'$	43.4001	57.0786
1	$1'$	8.5910	11.4184
2	$2'$	8.5812	11.4323
3	$3'$	8.5871	11.4257

Table 6

i	x_i[m]	y_i[m]	z_i[m]	φ_{ix}[rad]	φ_{iy}[rad]	φ_{iz}[rad]
0	-45.0000	0.0000	0.0000	0.0000	0.0000	0.0052
1	-30.0000	0.0740	-0.0004	0.0018	0.0000	0.0044
2	-15.0000	0.1270	-0.0007	0.0029	0.0000	0.0025
3	0.0000	0.1460	-0.0008	0.0032	0.0000	0.0000

Table 7

i	j	N	T_y	T_z	M_x	M_y	M_z
0	1	0.0047	-1.8056	0.0011	-3.6809	0.0000	0.0000
1	2	0.0010	-1.0120	-0.0000	-2.1633	0.0259	27.0311
2	3	-0.0058	-0.3127	-0.0005	-0.6996	0.0314	42.1557
3	4	-0.0058	0.3127	0.0005	0.6996	0.0240	46.8461

Conclusions

— Tie rods of each cable are acted upon by about equal forces (± 1 to $2\%_{00}$).

— Stress drop in tie rods of cable 1 is about 1% less than stress increase in tie rods of cable 2.

— Given horizontal load is balanced by three effects viz.: rigidity beam bending, secondary effect of initial stresses, and cable force variations, this latter being about constant for a node but the first two are rather different because of different tie rod inclinations (see Table 8). Secondary effect of initial forces balances 1.8% of the load at node 1, and 9.2% at node 3.

— Distances of nodes from planes passing through nodes 0', 3', 6' have been examined and compiled in cm in Table 9.

Table 8

Effect	Node	1	2	3
Rigidity beam		0.794	0.699	0.625
Initial stress		0.041	0.126	0.207
Cable force variation		1.415	1.425	1.418
Total [Mp]		2.250	2.250	2.250

Table 9

Node	Cable 1	Cable 2
1'	1.129	1.134
2'	0.638	0.641
1	5.464	5.452
2	0.812	0.813
3	0.856	0.850

— Even extension of the longest tie rod is less than 0.7 mm. Thus assumption of suspension sheet indeformability involves little error compared to displacements of ten-cm order.

Using the same data, the problem has been run by considering the rigidity beam as restrained in the horizontal plane ($\varphi_{z0} = \varphi_{z6} = 0$). Displacements and cable force variations were less than halved. For this case, displacements and stresses are shown in Tables 10 to 13 (corresponding to Tables 4 to 7).

3*

Table 10

i	Cable 1			Cable 2		
	x_i	y_i	z_i	x_i	y_i	z_i
0′	−45.0000	8.5101	−13.6333	−45.0000	−8.5101	−13.6333
1′	−29.9992	4.7812	− 7.1374	−30.0008	−4.7389	− 7.1388
2′	−14.9977	2.5554	− 3.2451	−15.0023	−2.4646	− 3.2368
3′	0.0000	1.8174	− 1.9474	0.0000	−1.7025	− 1.9365
1	−30.0017	0.7814	− 0.2094	−29.9983	−0.7386	− 0.2105
2	−15.0014	0.8144	− 0.2091	−14.9986	−0.7056	− 0.2108
3	0.0000	0.8287	− 0.2090	0.0000	−0.6913	− 0.2109

Table 11

i	j	Cable 1	Cable 2
0′	1′	52.8450	59.0020
1′	2′	49.3486	55.0950
2′	3′	47.5255	53.0094
1	1′	9.4754	10.5298
2	2′	9.4241	10.5872
3	3′	9.4153	10.5977

Table 12

i	$x_i[m]$	$y_i[m]$	$z_i[m]$	$\varphi_{ix}[\text{rad}]$	$\varphi_{iy}[\text{rad}]$	$\varphi_{iz}[\text{rad}]$
0	−45.0000	0.0000	0.0000	0.0000	−0.0000	0.0000
1	−30.0000	0.0213	0.0000	0.0007	−0.0000	0.0023
2	−15.0000	0.0542	0.0001	0.0011	−0.0000	0.0018
3	0.0000	0.0685	0.0001	0.0013	0.0000	0.0000

Table 13

i	j	N	T_y	T_z	M_x	M_y	M_z
0	1	0.0000	−4.1125	−0.0004	−1.4553	0.0000	−71.2449
1	2	0.0007	−2.3907	0.0002	−0.8804	−0.0042	− 9.5798
2	3	−0.0008	−0.7733	−0.0000	−0.2832	−0.0002	26.2511
3	4	−0.0008	0.7733	0.0000	0.2832	−0.0002	37.8508

Structural behaviour is best simulated by elastic restraint. Reliability of the output depends on the correct assumption of the spring constant.

At last, nodal displacements and stresses have been computed for twice the cable cross sections, with some typical outputs shown in Table 14 (confronted by corresponding values from both previous problems).

Table 14

	Dimension	EA = 13750 Mp $\varphi_{z_0} \neq 0$	EA = 13750 Mp $\varphi_{z_0} = 0$	EA = 27500 Mp $\varphi_{z_0} = 0$
Stress change in rod 3—3' of cable 1	Mp	−1.4129	−0.5847	−0.8930
Stress change in rod 3—3' of cable 2	Mp	1.4257	0.5977	0.9111
Rigidity beam midspan cross section displacements and stress u_{3y}	m	0.1460	0.0685	0.0556
φ_{3x}	rad	0.0032	0.0013	0.0021
M_{3z}	mMp	46.8461	37.8508	30.7433

Summary

Displacements and stresses in some suspended beams with rigidity beams and inclined cable planes have been determined, applying the first- or second- order theory for the rigidity beam, and the third-order theory for the cables. To this aim, an adequate computation method of the complementary rigidity matrix of the flexural, spatial rod has been presented.

References

1. VISONTAI, J.: Approximate Analysis of Suspended Beams with Rigidity Beams and Inclined Cable Planes.* Candidate's Thesis. Budapest, 1969. 182.
2. VISONTAI, J.: Approximative Analysis of Suspension Bridges with Cables in Inclined Planes. Per. Pol. C. E. Vol. 17. 1—2 Budapest, 1973. pp. 95—110.
3. SZABÓ, J.— KOLLÁR, L.: Analysis of Suspension Roofs.* Műszaki Könyvkiadó, Budapest 1974, pp. 95—110.
4. SZABÓ, J.—ROLLER, B.: Theory and Computation of Bar Systems.* Műszaki Könyvkiadó, Budapest 1971. 268.
5. GÁSPÁR, ZS.—ROLLER, B.: Some Problems of the Second-order Theory of Structures with Finite Freedom Degrees.* Építés—Építészettudomány IV. (3—4) Budapest, 1973. 373—394.

Dr. Zsolt GÁSPÁR, Research worker, H-1502 Budapest

* In Hungarian